

SANDIA REPORT

SAND2012-7665

Unlimited Release

Printed September, 2012

Nanofabrication of Tunable Nanowire Lasers via Electron and Ion-Beam Based Techniques

Qiming Li, George T. Wang, Jeremy Wright, Huiwen Xu, Ting-Shan Luk, Igal Brener, Jeffrey Figiel, Karen Cross, Mary H. Crawford, Stephen R. Lee, and Daniel D. Koleske

Prepared by
Sandia National Laboratories
Albuquerque, New Mexico 87185 and Livermore, California 94550

Sandia National Laboratories is a multi-program laboratory managed and operated by Sandia Corporation, a wholly owned subsidiary of Lockheed Martin Corporation, for the U.S. Department of Energy's National Nuclear Security Administration under contract DE-AC04-94AL85000.

Approved for public release; further dissemination unlimited.



Sandia National Laboratories

Issued by Sandia National Laboratories, operated for the United States Department of Energy by Sandia Corporation.

NOTICE: This report was prepared as an account of work sponsored by an agency of the United States Government. Neither the United States Government, nor any agency thereof, nor any of their employees, nor any of their contractors, subcontractors, or their employees, make any warranty, express or implied, or assume any legal liability or responsibility for the accuracy, completeness, or usefulness of any information, apparatus, product, or process disclosed, or represent that its use would not infringe privately owned rights. Reference herein to any specific commercial product, process, or service by trade name, trademark, manufacturer, or otherwise, does not necessarily constitute or imply its endorsement, recommendation, or favoring by the United States Government, any agency thereof, or any of their contractors or subcontractors. The views and opinions expressed herein do not necessarily state or reflect those of the United States Government, any agency thereof, or any of their contractors.

Printed in the United States of America. This report has been reproduced directly from the best available copy.

Available to DOE and DOE contractors from

U.S. Department of Energy
Office of Scientific and Technical Information
P.O. Box 62
Oak Ridge, TN 37831

Telephone: (865) 576-8401
Facsimile: (865) 576-5728
E-Mail: reports@adonis.osti.gov
Online ordering: <http://www.osti.gov/bridge>

Available to the public from

U.S. Department of Commerce
National Technical Information Service
5285 Port Royal Rd.
Springfield, VA 22161

Telephone: (800) 553-6847
Facsimile: (703) 605-6900
E-Mail: orders@ntis.fedworld.gov
Online order: <http://www.ntis.gov/help/ordermethods.asp?loc=7-4-0#online>



Nanofabrication of Tunable Nanowire Lasers via Electron and Ion-Beam Based Techniques

Qiming Li¹, George T. Wang¹, Jeremy Wright², Huiwen Xu¹, Ting-Shan Luk³, Igal Brener², Jeffrey Figiel¹, Karen Cross¹, Mary H. Crawford⁴, Stephen R. Lee⁴, and Daniel D. Koleske¹

¹Department of Advanced Materials Sciences (Org. 01126)

²Department of Nanostructure Physics (Org. 01131)

³Department of Applied Photonic Microsystems (Org. 01727)

⁴Department of Semiconductor and Optical Sciences (Org. 01120)

⁵Department of Semiconductor Material and Device Sciences (Org. 01123)

Sandia National Laboratories
P.O. Box 5800
Albuquerque, New Mexico 87185-MS 1086

Abstract

GaN nanowires were created from planar GaN epilayers using a top-down fabrication technique consisting of a dry etch followed by an anisotropic wet etch. The GaN nanowires are m-plane bounded with tightly-controlled dimensions. Single-mode lasing was achieved with GaN nanowire with 130 nm diameter and 5 μm length. Numerical simulations based on a multimode laser theory indicate that the suppression of transverse and longitudinal side-modes is caused by strong mode competition and narrow gain bandwidth. For multiple mode GaN nanowire lasers with large diameter, we demonstrated that coupled nanowire pairs provide a mode selection mechanism through Vernier effect and become single mode lasers. Moreover, transverse-mode suppression and single-mode lasing is demonstrated in GaN nanowires in contact with gold substrates, which introduces an attenuation effect to the cavity modes. The finite-difference time-domain simulations confirm the absorption effect, which give rise to a mode selection mechanism for realizing single mode operation.

ACKNOWLEDGMENTS

The nanowire fabrication was supported by Sandia's Laboratory Directed Research and Development program. The optical measurement was supported by Sandia's Solid-State-Lighting Science Energy Frontier Research Center, which is funded by the U. S. Department of Energy, Office of Science, Office of Basic Energy Sciences. This work was performed, in part, at the Center for Integrated Nanotechnologies, a U.S. Department of Energy, Office of Basic Energy Sciences user facility. Sandia National Laboratories is a multi-program laboratory managed and operated by Sandia Corporation, a wholly owned subsidiary of Lockheed Martin Corporation, for the U.S. Department of Energy's National Nuclear Security Administration under contract DE-AC04-94AL85000.

CONTENTS

1. INTRODUCTION	11
2. EXPERIMENTAL DETAILS	13
2.1. “Top down” GaN Nanowire Fabrication	13
2.2. GaN Nanowire Manipulation.....	14
2.3. Nanowire Material and Optical Characterization	15
2.4. Numerical Simulations.....	16
3. RESULTS AND DISCUSSIONS	17
3.1. DBR and DFB structure on nanowire using electron beam and focused ion beam direct write 17	
3.2. Single mode nanowire laser through geometry control	17
3.3. Single mode nanowire laser through couple cavities.....	20
3.4. Single mode nanowire laser through absorbing gold substrates	24
4. CONCLUSIONS	29
5. REFERENCES	31
Distribution	33

FIGURES

Figure 1. Cross sectional SEM images showing GaN posts morphology transiting into GaN nanowires (a) before wet etch, (b) after 2 hours, (c) after 6 hours and (d) after 9 hours from start of wet etch. All images have the same magnification.	14
Figure 2. Platinum DBR gratings cover both ends of a GaN nanowire. The scale bar represents 1 um.	15
Figure 3. The sidewall of a GaN nanowire is ion milled to form a periodical DBF grating.	15
Figure 4. Schematics of the GaN nanowire optical pumping and measurement setup.....	16
Figure 5. CCD images of a GaN nanowire pumped below (a) and above (b) lasing threshold, respectively. The nanowire laser emits a highly divergent beam from the facets, some of which is collected by the objective lens. The objective lens also collects radiation emitted from the facets that is scattered by the SiN substrate surface, as well as spontaneous emission exiting perpendicular to the nanowire axis.	17
Figure 6. (a, d) Nanowire laser intensity versus pump laser intensity, for two different nanowires with lengths of 4.7 μ m and 7.2 μ m (top and bottom, respectively). (c,f) Photoluminescence spectra from the nanowire lasers for pump intensities as indicated in the figures. (b,e) Scanning electron micrographs of the GaN nanowire lasers. (b) shows the smaller dimensioned nanowire with a width of 135nm and length of 4.7 μ m (e) shows the larger dimensioned nanowire with a width of 145nm and length of 7.2 μ m.	19

Figure 7. Emission spectra for 4.5 μm (a) and 7.3 μm (b) long nanowire lasers and different excitation, as indicated.....	20
Figure 8. (a) Individual GaN nanowires. The scale bar represents 10 micrometers. (b) The GaN nanowires was manipulated into a coupled nanowire cavity. The scale bar represents 5 micrometers.....	21
Figure 9. Lasing emission spectra of the coupled nanowire pair and corresponding separated individual nanowires. The three spectra were obtained with the same pump intensity of 1429 kW/cm ²	22
Figure 10. SEM image of partial overlapped two nanowires for verifying the evanescent coupling. The scale bar represents 3 μm . The inset is the CCD image when nanowire A was optically pumped.....	23
Figure 11. Calculated Transmission of the 7.8 and 8 μm cavities.....	23
Figure 12. Overlapping wavelengths for the nanowire-pair versus effective group refractive index. Three points nearest the gain spectrum are plot for each n_g . The shaded area indicates the gain bandwidth.....	24
Figure 13. Transverse modes supported by the nanowire-metal geometry. The black circle and straight line indicate the surfaces of the nanowire and metal substrate, respectively.....	25
Figure 14. Design of substrate for optical characterization of GaN nanowires. The inset shows the SEM image of gold spots evaporated on the SiN membrane.	26
Figure 15. SEM images of a nanowire on different substrates. (a) on SiN; (b) on Gold.....	27
Figure 16. Spectra of nanowire lasing on different substrates. (a) on SiN; (b) on gold.	27

TABLES

Table 1. Propagation loss for modes supported by the 300nm diameter nanowire.....	25
---	----

NOMENCLATURE

LED	Light Emitting Diode
SEM	Secondary Electron Microscopy (or Microscope)
FIB	Focused Ion Beam
DBR	Distributed Bragg Reflector
DFB	Distributed Feedback
XRD	X-ray Diffraction
PL	Photoluminescence
YAG	Yttrium Aluminum garnet ($Y_3Al_5O_{12}$)
CCD	Charged Couple Device
FDTD	Finite Difference Time Domain
FWHM	Full Width at Half Maximum
FSR	Free Spectrum Range

1. INTRODUCTION

There is a strong desire to reduce the volume of lasers to the minimum limit in order to enable ultra-compact and low-threshold coherent light sources. Such nanolasers could enable a host of impactful and diverse applications such as nanoscale optical interconnects, ultrahigh density data storage, nanolithography, quantum computing, cell probes, and chem-bio sensing. Advances in nanowire lasers are occurring at a rapid pace, with optically pumped lasers demonstrated in a variety of semiconductor material systems, including Group III-nitrides,[1], [2], [3], [4], [5], Group III-V[6], and Group II-VI.[7], [8] To achieve single-mode lasing, Xiao *et al.* used a CdSe active medium and a complex resonator comprising of coupled loops of long, flexible nanowires.[9] Recently, Scofield *et al.* reported single-mode lasing from a defect mode in an InGaAs photonic crystal consisting of a 2-dimensional array of InGaAs nanowires.[10] To circumvent the need for fabrication and manipulation of complicated optical structures, we concentrated our effort towards a simple, linear, Fabry-Perot nanowire laser, where the factors enabling single-mode lasing are short cavity length, small cross section and very high material gain. By reducing the nanowire size, the number of cavity modes within the gain bandwidth is dramatically reduced. This in turn requires high material gain, necessary to compensate for the reduced gain length. Low defect density and high sample uniformity are also necessary to reduce carrier losses and inhomogeneous broadening, in order to achieve high carrier density and increase gain competition, respectively. By satisfying these requirements, we are able to demonstrate single-mode lasing with a linewidth of ~ 0.12 nm and >18 dB side-mode suppression ratio, in a 135nm wide, 4.7 μ m long GaN nanowire, under optical pumping. Single-mode operation is maintained far above lasing threshold. With GaN (or InGaN), the payoff is single-mode laser operation at ultraviolet (or green) wavelengths, which is an important spectral region not covered well by present semiconductor lasers.

2. EXPERIMENTAL DETAILS

2.1. “Top down” GaN Nanowire Fabrication

To achieve single mode lasing, precise control over the nanowire geometry is required. This requirement is satisfied by a top-down fabrication technique which produces uniform and vertically aligned GaN nanowire arrays from *c*-plane GaN epilayers on sapphire with low defect density and smooth sidewalls. We previously demonstrated this technique to fabricate nanowire LED structures with an axial GaN/InGaN multi-quantum structure.[11] Figure 1 shows SEM images of top-down GaN nanowires during the fabrication process. Starting from Si-doped planar GaN epilayers grown on 2” *c*-plane sapphire wafers in a Veeco D-125 metal organic chemical vapor deposition reactor, a 2-step etching process is used: a lithographic dry etch followed by an anisotropic wet etch. Following a process reported by Reculosa and Ravaine, a monolayer of 3 μm diameter silica colloids was self-assembled on the GaN surface in a Langmuir-Blodgett trough prior to etching to serve as a semi-periodic lithographic etch mask. GaN posts are subsequently formed by a plasma (dry) etch. As shown in Fig. 1 (a), the resulting posts are tapered with large cross-section areas, and therefore, are unsuitable for single-mode nanowire lasers. Moreover, ion bombardment during the plasma etch damages the nanowire surface, as evidenced by significant increase in yellow luminescence.[12] These issues are resolved during the second (wet) etch step [Figs. 1 (b) - (d)]. With the anisotropic wet-etch step, non-tapered GaN nanowires are created with damage-free surfaces, hexagonal cross sections, and well-defined resonator facets. The GaN nanowire length is determined by the original GaN epilayers thickness and its width is determined by the duration of the wet-etch.

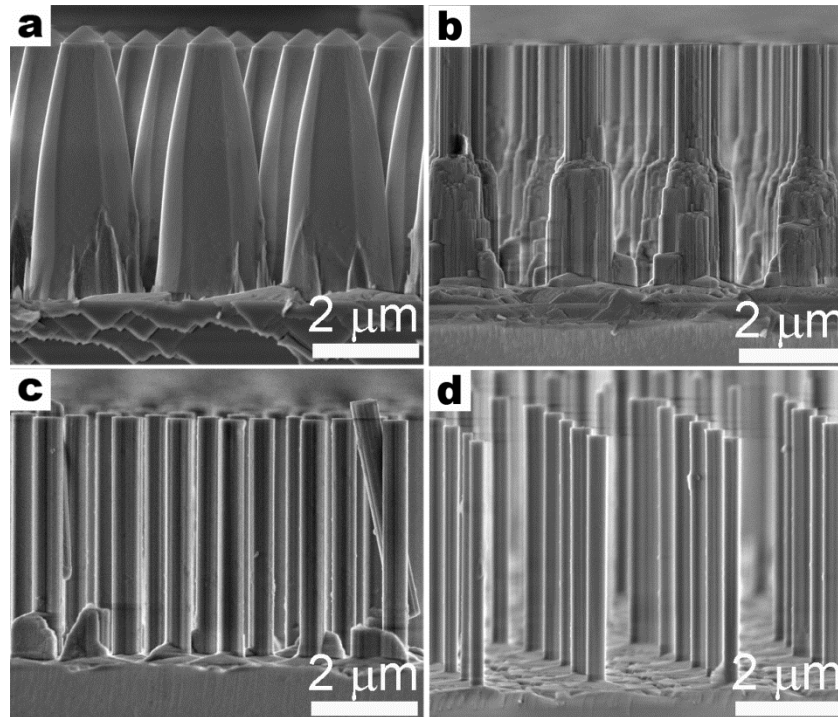


Figure 1. Cross sectional SEM images showing GaN posts morphology transitioning into GaN nanowires (a) before wet etch, (b) after 2 hours, (c) after 6 hours and (d) after 9 hours from start of wet etch. All images have the same magnification.

2.2. GaN Nanowire Manipulation

The SEM systems we used to study GaN nanowire are equipped with FIB, metal organic compound precursor gas nozzle, and a pair of piezoelectric motor driven nano-manipulators. FIB and the gas nozzle allow us to create DBR and DFB features on GaN nanowire. Figure 3 shows a SEM image of a GaN nanowire with both ends covered by platinum gratings. Each set of the platinum gratings consist of 5 parallel 30-nm-thick and 1.5-um-long platinum nanowire wires. The spacing between the nanowire is 75 nanometers. Figure 4 shows a SEM image of a GaN with its side wall milled by programmed FIB. The formed trenches have 75 nm in pitch.

The nano-manipulators in the SEM allow us to arrange or position GaN nanowires according a specific design. In this case, we use the nano-manipulators to push two individual nanowires to contact each other to form a coupled pair. We also move GaN nanowire from initial silicon nitride surfaces to gold patches, which are formed by lithography, gold evaporation, and liftoff.

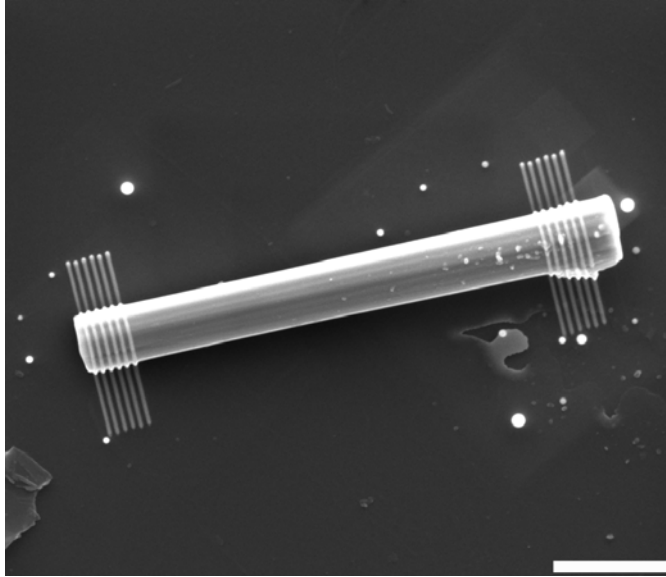


Figure 2. Platinum DBR gratings cover both ends of a GaN nanowire. The scale bar represents 1 μm .

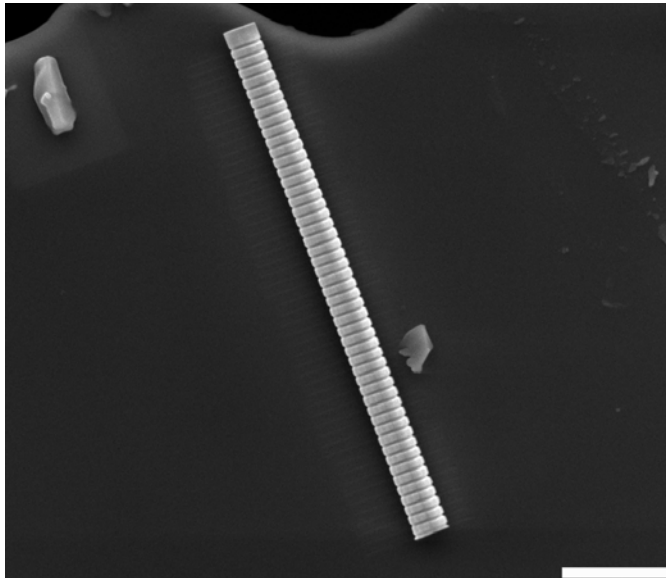


Figure 3. The sidewall of a GaN nanowire is ion milled to form a periodical DBF grating.

2.3. Nanowire Material and Optical Characterization

The nanowires were characterized by scanning electron microscopy (SEM), x-ray diffraction (XRD) and transmission electron microscopy (TEM). For the optical pumping measurements, the nanowires were removed from their sapphire growth substrate and transferred to clean SiN surfaces on TEM grids. Each nanowire was optically pumped at room temperature with a 266 nm pulsed quadrupled YAG laser emitting at 247nm. The intensity incident on the nanowire was varied using neutral density filters. A 50 \times ultraviolet objective lens is used to image the pump laser output to an approximately 5 μm diameter spot on the GaN nanowire. Optical emission

from the nanowire was collected with the same objective lens. The collected light was analyzed by a cooled CCD detector and a 300 mm spectrometer with a 2400 groove/mm holographic grating. The schematic of the optical pumping measurement set up is given in Figure 2.

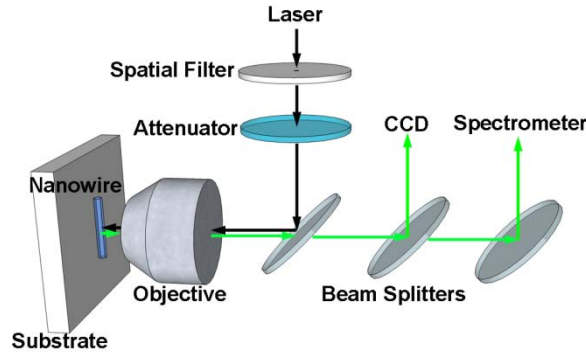


Figure 4. Schematics of the GaN nanowire optical pumping and measurement setup.

2.4. Numerical Simulations

First, the nanowire passive-cavity eigenmodes are determined using a finite-difference time-domain (FDTD) solver. To determine which of the passive-cavity modes will be lasing, the FDTD information is fed into a laser model. We use a semiclassical multimode laser model, where the time evolution of the intensity I_n in a passive-cavity mode n is given by[13]

$$\dot{I}_n = \left(\alpha_n - \beta_n I_n - \sum_{m \neq n} \theta_{nm} I_m \right) I_n + F$$

In the above equation, α_n is the net modal gain, β_n is the self saturation coefficient, θ_{nm} is the cross-saturation coefficient, F accounts for spontaneous emission and the summation $\sum_{m \neq n}$ is over all passive-cavity modes in the nanowire. The equation resembles closely the Lotka-Votterra equations, which is widely used for describing predator-prey dynamics in biological systems. Modifications to the typical multimode laser analysis include a more accurate treatment of outcoupling effects by coupling the nanowire cavity to free space.[14] Doing so allows the description of line narrowing of each passive cavity model as the device makes the transition from below to above lasing threshold. The GaN gain medium parameters for different frequencies and carrier densities, such as the net modal gain α_n , are determined from a many-body gain theory.[15]

The set of coupled mode intensity equations (numbering roughly 300) is solved numerically for the steady-state solution for a given excitation level, α_1/β_1 . Plotting the steady-state I_n versus the passive cavity-mode frequency Ω_n gives the emission spectrum.

3. RESULTS AND DISCUSSIONS

3.1. DBR and DFB structure on nanowire using electron beam and focused ion beam direct write

The DBR and DFB structures were created by electron beam and focused ion beam direct write, as shown in Figure 2 and 3. The PL of the nanowires with these features was completed quenched after the beam assisted processes. This result indicates that the GaN materials are no longer optically active. We speculate that during the electron beam assisted metal deposition, a thin layer of metal probably cover the surfaces of the GaN nanowire and cause the absorption of the optical pump energy as well as free carriers if any. Moreover, for the nanowire treated by FIB, as shown in Figure 3, the energetic ($\sim 30\text{KeV}$) Ga ions may damage the lattice sites and create point defects, which are known to negatively impact the band edge emission of GaN.

3.2. Single mode nanowire laser through geometry control

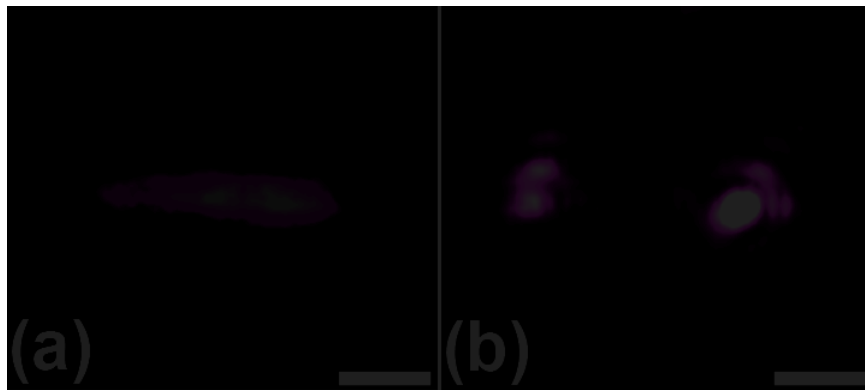


Figure 5. CCD images of a GaN nanowire pumped below (a) and above (b) lasing threshold, respectively. The nanowire laser emits a highly divergent beam from the facets, some of which is collected by the objective lens. The objective lens also collects radiation emitted from the facets that is scattered by the SiN substrate surface, as well as spontaneous emission exiting perpendicular to the nanowire axis.

The optical properties of the GaN nanowires were characterized by optical pumping using a micro-photoluminescence setup as sketched in Figure 4. For comparison, two nanowires of similar diameters but different lengths were fabricated and characterized. A 135nm diameter, 4.7 μm long nanowire and a 145nm diameter, 7.2 μm long nanowire were positioned on SiN substrates. Figures 5 (a) and (b) show CCD images of optical emission from the shorter GaN nanowire at two pump intensities. At low pump intensity, the CCD image shows roughly uniform optical emission from the entire nanowire length, indicating that unguided (out-of-plane) and guided (on-axis) emission intensities are basically equal [see Figure 5(a)]. The inference is that the optical emission is entirely from spontaneous emission. At higher pump intensity, a distinctly different emission pattern emerges. The on-axis emission grows significantly, appearing as two bright spots at the ends of the nanowire indicative of Fabry-Perot lasing, as shown in Figure 5 (b). The light collected by the objective lens is directly from the highly

diverging output beam and indirectly from scattering of the output beam by the SiN surface. The large divergence angle of output beam is because of diffraction from a sub-wavelength nanowire aperture. At the same time, there is a clamping of the unguided spontaneous emission, which appears as a darkening (relative to the bright ends and with filters in place) of the entire length of the nanowire, also shown in Figure 5(b). Also present in the CCD image are concentric rings of optical interference fringes, which is an indication of the spectral coherence of the emitted light.

Figure 6 plots the light out versus pump power and output intensity spectra for the two nanowire lasers of different lengths. The experiment was performed at $T = 300$ K. For both nanowires, the light out versus pump power curves show abrupt slope changes indicative of lasing threshold. Also, the peak intensity grew linearly with no sign of saturation throughout the excitation range. Emission spectra were measured at various pump intensities. The right column shows spectra for the two nanowire lasers at four optical pumping intensities. For the $4.7\mu\text{m}$ long nanowire laser, the emission spectrum (lowest curve, Figure 6(c)) is featureless and broad, with a full-width at half-maximum (FWHM) of approximately 6 nm at a pump intensity of $150\text{kW}/\text{cm}^2$. At the next higher pump intensity of $268\text{kW}/\text{cm}^2$, the emission spectrum starts to exhibit many sharp peaks, suggesting the onset of amplified spontaneous emission. For a pump intensity of $323\text{kW}/\text{cm}^2$, the spectrum shows a single sharp peak with $\text{FWHM} < 0.12$ nm over a broad background. The single-mode behavior remains (see highest intensity spectrum, Figure 6(c)) as the pump intensity continues to increase. For this laser, the mode spacing was measured to be 1.9nm . Side-mode suppression ratio is also maintained at greater than 18dB . An increase in the nanowire length results in a significant reduction in side-mode suppression, leading to emission characteristic of multimode lasing, as evidenced by the $7.2\mu\text{m}$ long nanowire shown in Fig. 4f. For this laser, the mode spacing was measured to be 1.3nm . We note that multimode lasing was typical for the larger diameter nanowires (e.g. $> \sim 180$ nm), with < 1.5 nm measured mode spacing.

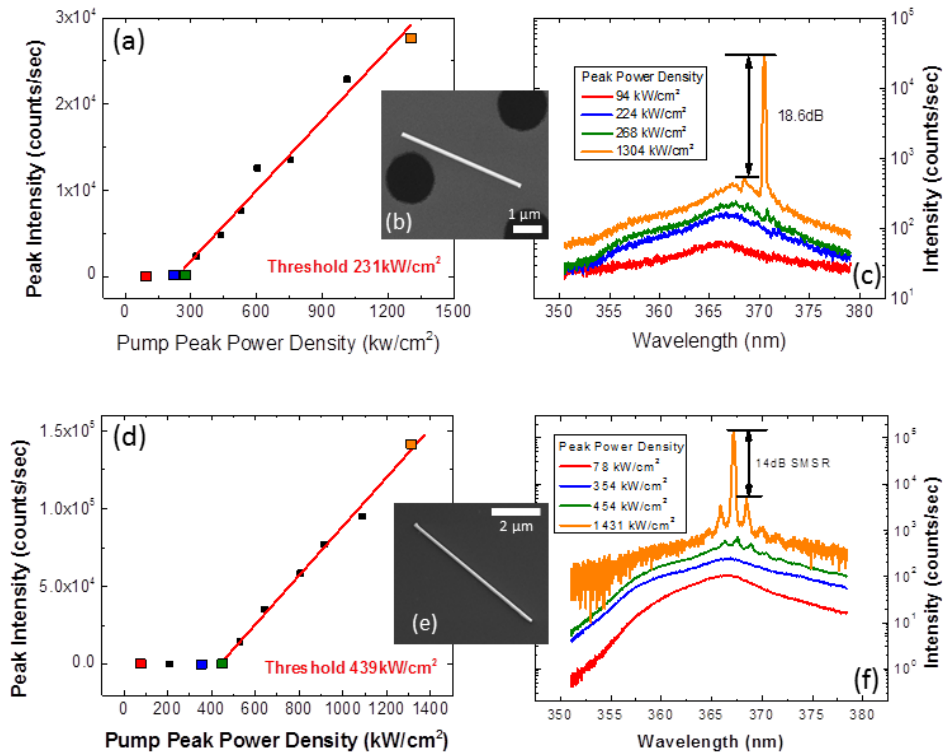


Figure 6. (a, d) Nanowire laser intensity versus pump laser intensity, for two different nanowires with lengths of 4.7 μm and 7.2 μm (top and bottom, respectively). (c,f) Photoluminescence spectra from the nanowire lasers for pump intensities as indicated in the figures. (b,e) Scanning electron micrographs of the GaN nanowire lasers. (b) shows the smaller dimensioned nanowire with a width of 135nm and length of 4.7 μm (e) shows the larger dimensioned nanowire with a width of 145nm and length of 7.2 μm .

Summarizing the experimental results at this point, Figs. 3 and 4 together provide strong evidence of single-mode lasing. Figure 5 (b) shows the clamping of spontaneous emission and interference fringes indicating coherence in optical emission.[16] There is the presence of a lasing threshold [Figure 6 (left column, top)] and spectral narrowing to single frequency [Figure 6 (right column, top)].

The experiments were modeled to better understand the mechanisms leading to single-mode lasing and to develop an analytical tool for designing future nanowire lasers. A combination of mode simulations, multimode-laser modeling and many-body laser-gain calculation were employed. First, the nanowire passive-cavity eigenmodes were determined using a full vectorial commercial mode solver from Lumerical Inc.. Then, multimode semiclassical laser theory[15] and many-body gain[15] calculations were used to determine which of the passive-cavity eigenmodes will be above lasing threshold for given experimental conditions. Emission spectra at different excitations were computed for nanowire lasers with dimensions approximating those experimentally measured. Figure 7 (a) shows the intensity spectra for increasing excitation for a 140 nm diameter, 4.5 μm long nanowire. The spectra show multiple resonances initially, which condense to only one mode operating above lasing threshold. A criterion for lasing is spectral line narrowing, as clearly exhibited by the mode at 363nm. On the other hand, each side mode

remains broader than the central mode, with width determined by the passive Fabry-Perot resonance. Amplified spontaneous emission gives rise to the side-mode intensity. Figure 7 (b) shows the case of a longer 7.3 μm long (140 nm diameter) nanowire laser. Side-mode suppression is decreased by roughly a factor of 3 when compared to the shorter nanowire laser for $\alpha_1/\beta_1 > 1$, where α_1 is the net modal gain and β_1 is the self saturation coefficient. Convincing evidence for multimode operation is from side-mode spectral narrowing to width comparable to the central mode, indicating that they are above lasing threshold. Fig. 5 is qualitatively consistent with the experimental results described in Fig. 4. Simulations were also performed for longer nanowire devices. We found multimode operation for lasers longer than ~ 7 μm , consistent with earlier reports and experiments performed at Sandia.

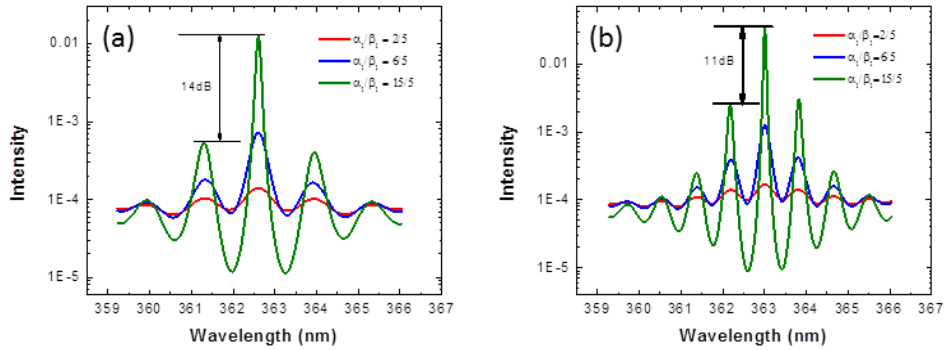


Figure 7. Emission spectra for 4.5 μm (a) and 7.3 μm (b) long nanowire lasers and different excitation, as indicated.

The value of the above modeling exercise is three-fold. First is a better understanding of the mechanisms giving rise to single-mode lasing. According to the multimode laser model, single-mode lasing depends on two factors: (1) suppression of modes (e.g. transverse modes) close to the single lasing mode via mode competition, and (2) absence of net gain in the further lying modes because of large longitudinal mode spacing and finite gain bandwidth. The second purpose of the model is to determine the laser parameters necessary for using the multimode laser model to design future lasers. Most important is the determination of the mode-coupling parameter,[17] $C \equiv \theta_{nm}\theta_{mn}/(\beta_n\beta_m)$, which is extremely difficult to obtain from first-principles because of complicated many-body correlation effects. Theory/experiment comparisons with different length nanowire lasers gives $0.7 < C < 1.0$, putting the GaN active medium in the upper end of the weak-coupling regime. Consequently, suppression of side modes comes entirely from the effective net gain $\alpha_n - \theta_{nm}\alpha_m/\beta_m < 0$ which gives rise to the condition of longitudinal mode space > 10 meV and $\Gamma_T/\Gamma_L < 0.9$ for single-mode lasing, where Γ_T and Γ_L are transverse and longitudinal mode confinement factors, respectively. Further study is necessary to confirm these conditions. The third value of the modeling is to provide information on the laser gain and carrier density achieved in our experiments. We estimated material gain and carrier density created under optical pumping to be $\approx 5.8 \times 10^3 \text{ cm}^{-1}$ and $1.4 \times 10^{19} \text{ cm}^{-3}$, respectively, which are appreciably higher than found in conventional lasers and is evidence for high material quality.

3.3. Single mode nanowire laser through couple cavities

Figure 8(a) shows a SEM image of two individual nanowires A and B with diameter/length of 680 nm/7.6 μm and 720 nm/8.0 μm , respectively. A typical PL spectrum pumped below threshold (from nanowire A) is shown as the inset in Figure 9. It is seen that the spectrum covers a range of ~ 20 nm with a full width at half maximum (FWHM) of 7.4 nm. At this low pump level, the corresponding CCD image of the nanowires showed a uniform emission from the entire body of the nanowires, indicating a weak cavity effect.[18] When pumped above lasing threshold, the individual nanowires displayed many salient features evidencing lasing behavior. The first feature is an interference pattern generation in the CCD image. The lasing of the nanowire can be considered as the emission of two closely-spaced coherent point-sources due to the strong diffraction at the two nanowire facets. The interaction of the two point-source emission forms the interference pattern, which provides an indicator of nanowire lasing. Details about the generation of these interference patterns in the GaN nanowires have been shown in our recent report¹³. The second feature is the sudden narrowing of the nanowire emission spectrum width from 7 nm to 0.14 nm, as shown in Figure 9. (red curve).

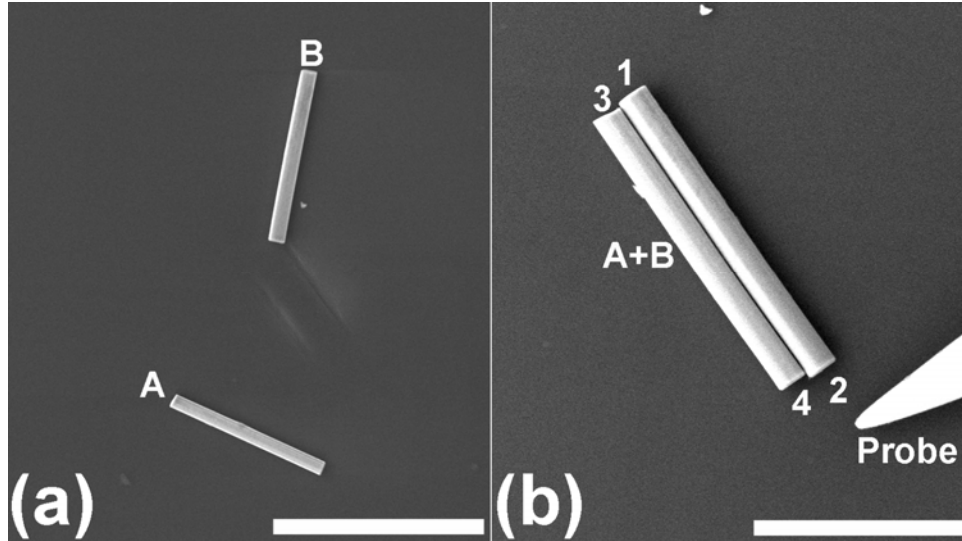


Figure 8. (a) Individual GaN nanowires. The scale bar represents 10 micrometers. (b) The GaN nanowires was manipulated into a coupled nanowire cavity. The scale bar represents 5 micrometers.

The lasing behavior of the individual GaN nanowires shows multiple transverse/longitudinal modes. This feature is evidenced by the uneven spacing between the lasing peaks. For a nanowire to function as a single-mode waveguide, the nanowire geometry should satisfy $(\pi D / \lambda)(n_1^2 - n_0^2)^{0.5} < 2.405$, [7] where D is the nanowire diameter, λ is the wavelength in vacuum, and n_1 and n_0 are the refractive indices of the nanowire and the surrounding air, respectively. From this equation, we calculated the critical diameter to be ~ 120 nm for a GaN nanowire to function as a single transverse-mode waveguide. Therefore, for a GaN nanowire with a diameter of ~ 700 nm, the lasing will be dominated by multi-transverse modes. For each transverse mode, a set of longitude modes is activated with the free spectral range (FSR) determined by $\Delta\lambda_{FSR} = \lambda^2 / 2n_g L$, with λ , L , n_g representing wavelength in vacuum, cavity length, and group refractive index, respectively. Therefore, multiple transverse modes give rise to multiple sets of longitude modes with different FSRs, because n_g varies with different transverse modes. The

overlapping of all sets of longitude modes leads to an uneven spectral map for possible lasing wavelengths. In addition, mode competition[19] and the spatial hole-burning effect[20] selectively support certain modes and shape the uneven-spaced lasing spectrum. We note that the spectral spacing shown in Figure 9 is much smaller than the predicted FSR of ~ 1.53 nm for a single transverse-mode operation (using $n_g=5.6$ [21], $D=370$ nm and $L=8$ μm for the calculation), which further verifies the multiple transverse-mode operation of the laser.

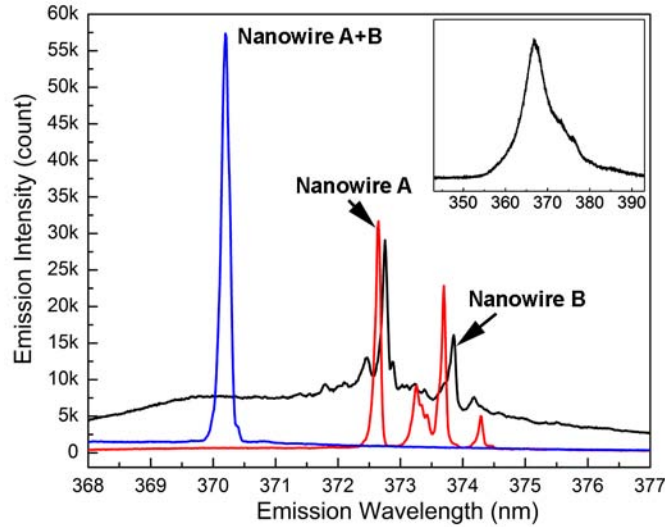


Figure 9. Lasing emission spectra of the coupled nanowire pair and corresponding separated individual nanowires. The three spectra were obtained with the same pump intensity of 1429 kW/cm^2 .

The coupled cavity formed by these two nanowires is shown in Fig. 1(b). Below lasing threshold, the PL emission from the nanowire pair was similar to that of an individual nanowire, showing a wide-band spectrum. However, above threshold, the nanowire pair exhibited single-mode lasing properties. As the pump intensity increased to 874 kW/cm^2 , a single sharp peak emerged from the wide-band PL background. Further increase of the pump intensity led to a corresponding increase of the spectral peak and a larger signal-to-noise ratio. The blue curve in Fig. 2 shows a typical spectrum of the single-wavelength lasing at a pump intensity of 1429 kW/cm^2 . It is seen that the lasing peak is located at 370 nm with a side mode suppression ratio (SMSR) of ~ 15.6 dB. Lorentzian fitting of the spectrum gives a FWHM of ~ 0.14 nm. The lasing was stable with no spectral mode-hopping observed. The lasing threshold of the nanowire-pair is 874 kW/cm^2 , which is comparable for that of each individual nanowire.

The simultaneous suppression of both multiple transverse and longitudinal mode operation for the coupled nanowires originates from a mode selection mechanism enabled by evanescent interaction between the two nanowires. Energy transfer through evanescent coupling has been demonstrated²⁰ and modeled²¹ for closely located nanowires. To verify the coupling effect in our nanowire-pairs, we shortened the overlapping length of two nanowires, and then selectively pumped one nanowire and observed the emission from the other one. To prevent the two nanowires from being pumped simultaneously, the spatial filter with a pump spot of $\sim 1 \mu\text{m}$ was utilized. As shown in Figure 10, when one end of nanowire A2 was pumped, the emission was observed from the bottom end of B2, as evidenced by the CCD image shown in the inset. This

result evidences that the light is able to transfer between the two nanowires, verifying the effective coupling effect. This coupling effect transforms a nanowire pair into a coupled cavity. In this coupled cavity, a set of resonance conditions has to be satisfied, i.e. simultaneous oscillation of each sub-cavity[9, 17, 22, 23]. In the nanowire pair cavity shown in Figure 8 (b), the new resonance condition is the simultaneous oscillation of four sub-cavities of 12 , 14 , 23 , and 34 . Since $L_{12} + L_{34} = L_{14} + L_{23}$ and $L_{13} = L_{24}$, the resonance condition will be simplified to the simultaneous oscillation of sub-cavity 12 and 14 .

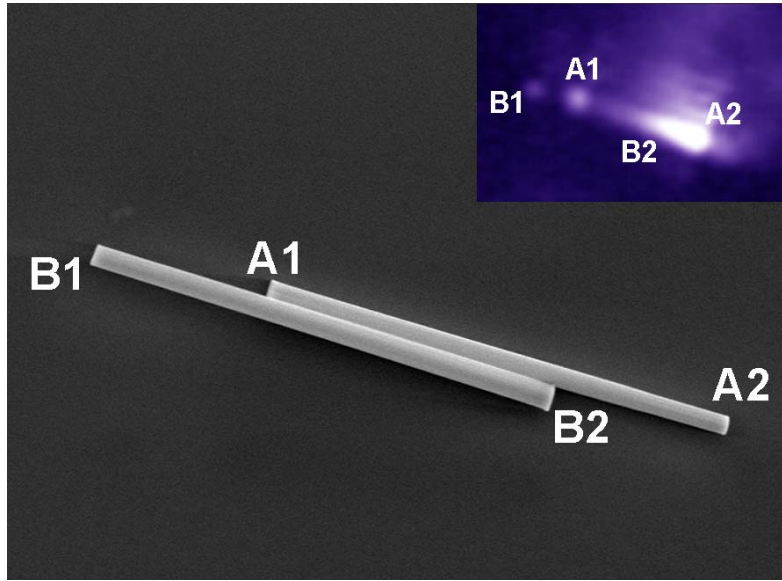


Figure 10. SEM image of partial overlapped two nanowires for verifying the evanescent coupling. The scale bar represents 3 μm . The inset is the CCD image when nanowire A was optically pumped.

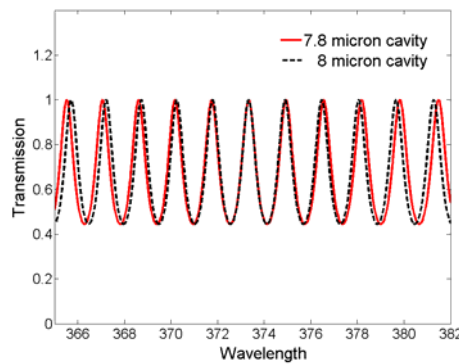


Figure 11. Calculated Transmission of the 7.8 and 8 μm cavities.

Since the diameters of the GaN nanowires are much larger than their emission wavelengths, in each sub-cavity many transverse modes exist with different value of group refractive index (n_g) ranging from 5.0-6.0[21]. For each of these transverse modes, the longitudinal modes can be expressed using

$$T(\lambda) = (1-R)^2 / \left[(1-R)^2 + 4R \sin^2(2\pi L n_g / \lambda) \right],$$

where T is the transmission of cavity, L is the nanowire length, n_g is the group refractive index, and R is the reflectivity at each nanowire facet ($R = (n - n_0 / n + n_0)^2 \approx 0.2$ when refractive index $n=2.6$ [21]). From this equation, the resonant wavelengths of longitude modes for each sub-cavity can be calculated. These resonant wavelengths are compared to determine overlapping resonant wavelengths between sub-cavity 12 (8 μm cavity) and 14 (7.8 μm cavity) as shown in Figure 11. It is seen that the modes of these two sub-cavities overlaps at ~ 373.3 nm and start to deviate from each other when the wavelength is shifted. Moreover, this calculation reveals that the spectral range of two overlapping wavelengths of the coupled nanowire cavity is about 50 nm, much larger than the gain bandwidth. Therefore, the overlapping mode at 373 nm is likely the only possible lasing mode for the coupled cavity. Note that this calculation assume a transverse mode with $n_g=5.6$. As n_g varies with different transverse modes, the overlapping mode may shift away from the gain range (approximately GaN emission range) and not oscillate. In other words, only the transverse mode with proper n_g can be selected by the coupled nanowire cavity. Figure 12 shows the calculated resonant wavelengths of the coupled cavity as n_g varies from 5.0 to 6.0. For each n_g , three overlapping resonant wavelengths near the gain are plotted in the figure. It is seen that there exists a resonant wavelength located within the gain band only when n_g is in the range from 5.47 to 5.64. Therefore, the coupled nanowire cavity provides a mechanism for selecting a transverse mode and thus functions as a single transverse mode laser.

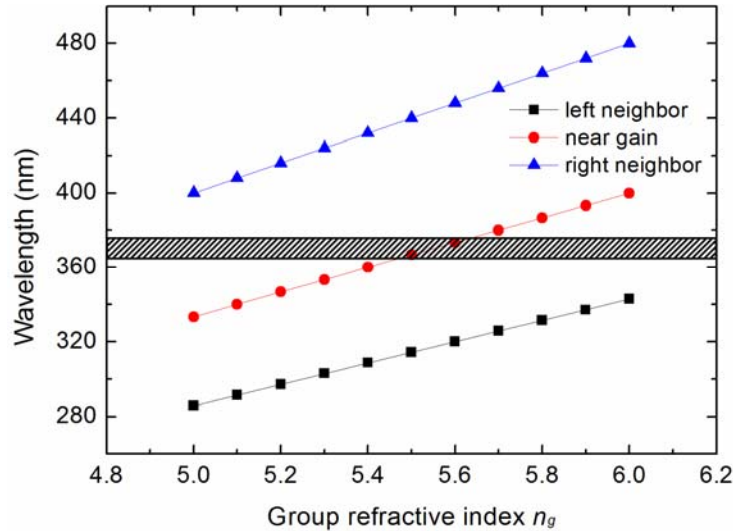


Figure 12. Overlapping wavelengths for the nanowire-pair versus effective group refractive index. Three points nearest the gain spectrum are plot for each n_g . The shaded area indicates the gain bandwidth.

3.4. Single mode nanowire laser through absorbing gold substrates

We developed another transverse-mode selection technique by using an absorptive material to serve as the nanowire substrate. Due to the moderate ohmic loss in the ultra-violet band, gold can be the proper substrate material. Note that the plasmonic frequency of gold is much higher than the GaN emission wavelength, which define our nanowire lasing as dielectric lasing, differing with the reported plasmonic lasing where metal layers were also utilized as substrates. Through the ohmic contact, an extra cavity loss can be expected. Moreover, due to the difference in the spatial distributions, the cavity loss should vary with different transverse modes, thereby generating the mode-sensitive loss.

To verify the mode-sensitive loss, we conducted finite-difference time-domain (FDTD) simulations to illustrate the gold substrate effects on the lasing properties of GaN nanowires. The nanowire passive cavity eigenmodes were determined using a full vectorial commercial mode solver from Lumerical Inc, which has been widely used to analyze mode distribution, frequency response, and propagation loss of nanoscale waveguides. In simulation, a cylindrical nanowire is defined on top of a $10\mu\text{m}\times 1.25\mu\text{m}\times 200\text{nm}$ (length \times width \times thickness) gold membrane. The refractive index of GaN is set as 2.6, and the real part and imaginary part of gold were set as 1.70 and 1.88 (typical values at $\sim 370\text{nm}$) respectively. The transverse modes supported by this geometry is analyzed by a cross section calculation, where 200 unit cells in both x and y directions are employed to ensure the accuracy of the simulation. The dimension of the nanowires can be modified readily to study the substrate effect on nanowires with different geometry.

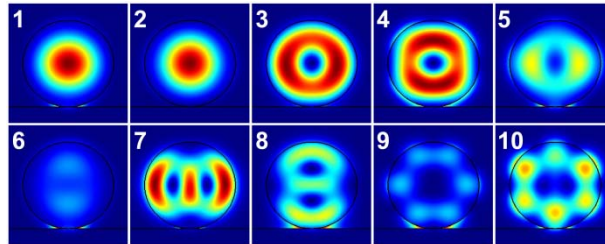


Figure 13. Transverse modes supported by the nanowire-metal geometry. The black circle and straight line indicate the surfaces of the nanowire and metal substrate, respectively.

Table 1. Propagation loss for modes supported by the 300nm diameter nanowire.

	Mode 1	Mode 2	Mode 3	Mode 4	Mode 5
Loss (dB/cm)	8151	1730	4806	7109	16041
	Mode 6	Mode 7	Mode 8	Mode 9	Mode 10
Loss (dB/cm)	34858	7551	22205	29175	28706

Figure 13 shows transverse mode distributions supported by a 300nm nanowire with the gold substrate. It is seen that ten modes are supported by the geometry. Due to the presence of the metal substrate, the mode degeneracy is broken, with modes in each order showing different polarization, mode distribution, and propagation loss. Table 1 shows the propagation loss of different modes from the simulation results. It is seen the propagation loss is sensitive to mode distribution, where more absorption will be generated for the modes of more overlapped area

with the substrate. Mode 2 has a smallest propagation loss of 1730dB/cm (corresponding to an extra 1.83dB or 34.4 percent cavity loss for a 5.3 μ m nanowire cavity), much less than those of all the other modes (Mode 3 has the second smallest loss of 4806dB/ μ m, corresponding to an extra 5.09dB or 84.7 percent cavity loss for a 5.3 μ m nanowire cavity). Therefore, single transverse-mode lasing can be ensured since Mode 2 will be the only mode capable of oscillating within the cavity. Further simulations have also been conducted for nanowires with different diameters, and it is found that higher losses will be generated with reduced nanowire diameter, and on the contrary, lower losses will be obtained with larger nanowire diameter. But in all these cases, a mode-dependent loss can always be obtained. Moreover, we find that nanowires with diameter ranging from 250 to 400nm are suitable for generating single transverse-mode operation since one specific mode experiences much less attenuation than others.

Guided by the simulation results, we fabricated nanowires with proper geometry for single-mode lasing operation. The GaN nanowires was fabricated by a top-down etch technique, as detailed in [24]. This technique is able to produce vertically aligned nanowire arrays from c-plane GaN epilayers with low defect density and smooth sidewalls. Briefly, A self-assembled and hexagonal close-packed monolayer of silica microspheres was firstly deposited onto the GaN epilayer to serve as a semi-periodic lithographic etch mask. A followed plasma etch was employed to generated nanopillars with large diameter and tapered shape. Eventually uniform GaN nanowires was achieved with a uniform surface after a further anisotropic wet etch. The GaN nanowire length is determined by the original GaN epilayers thickness and its width is determined by the duration of the wet-etch. Nanowires were intentionally fabricated with ~300nm diameter and ~5.3 μ m length for the purpose of verifying the simulation results and bypassing the multiple longitude-mode oscillation, respectively. These nanowires were then transferred to an elaborately prepared substrate for optical characterization. The structure of the substrate is sketched in Figure 14. The substrate is a 300nm-thick Si₃N₄ membrane selectively coated with 200nm-thick gold spots. The lasing properties of nanowires on the Si₃N₄ membrane were firstly studied. Then these nanowires were transferred onto the gold substrate by a peizo-electric platinum nanoprobe, and their lasing behavior was studied as well for comparison.

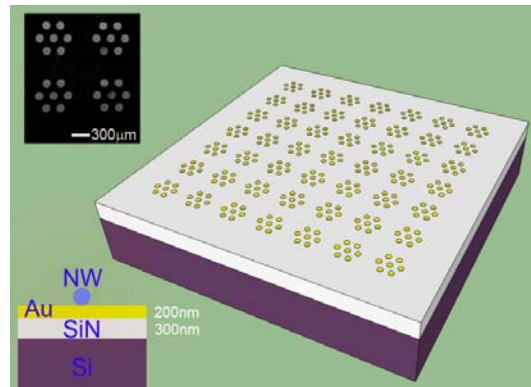


Figure 14. Design of substrate for optical characterization of GaN nanowires. The inset shows the SEM image of gold spots evaporated on the SiN membrane.

The optical properties of the nanowire were characterized using a micro-photoluminescence setup. The pump laser were a frequency-quadrupled Nd:YAG laser operating at 266nm with a

pulse duration of 400ps and a repetition rate of 10 kHz. The nanowire was excited using the pulsed laser through a 50× ultraviolet objective with a 5μm spot size, and the emission from the nanowire was collected by the same objective and analyzed using a CCD detector and a 300 mm spectrometer with a 1200 groove/mm holographic grating.

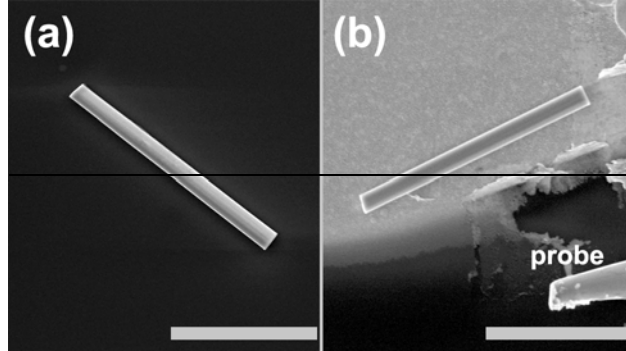


Figure 15. SEM images of a nanowire on different substrates. (a) on SiN; (b) on Gold. The scale bars represent 3mm.

Figure 15(a) shows the scanning electron microscopic (SEM) image of a nanowire on the Si₃N₄ substrate. The nanowire is measured to be ~350nm in diameter, and 5.3μm in length. Below threshold, the nanowire showed a broadband photoluminescence (PL) emission, with the spectrum centered at 367.5nm and a full-width half-maximum of ~7.5nm. A lasing threshold of 241kW/cm² was obtained by gradual increase of the pump power. Figure 16(a) shows the typical lasing spectra at different pump levels. The blue curve shows a spectrum when the nanowire was pumped slightly below threshold. It is seen several peaks appear in the spectrum. Corresponding to the increase of the pump intensity, most of these peaks grew up simultaneously with an enhanced signal-to-noise ratio, accompanied with the emergence of some new resonant peaks, as shown in the red spectral curve. The black curve shows the spectrum when the pump power was 458KW/cm². Six dominating peaks are seen in the spectrum with an uneven spectral spacing. A minimum spacing of ~0.58 nm is observed, much smaller than the calculated longitudinal mode spacing of ~2.1nm for a single transverse-mode operation. All these spectral features indicate the multiple transverse-mode operation of the nanowire laser.

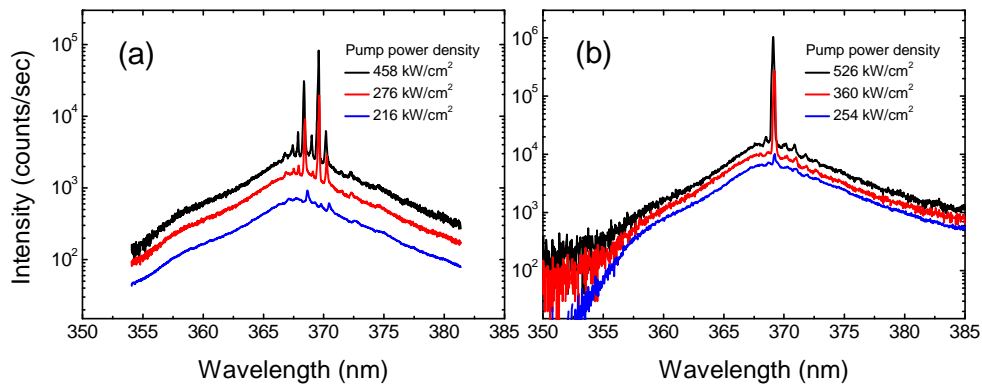


Figure 16. Spectra of nanowire lasing on different substrates. (a) on SiN; (b) on gold.

Significant transverse-mode suppression was realized when the nanowire was transferred to the gold substrate. Figure 15 shows the SEM image of the same nanowire on the gold membrane. Under gradually increased optical pumping, similar spectral evolution from PL to lasing has been observed. Due to the extra cavity loss introduced by the metal substrate, the lasing threshold has increased to $276\text{KW}/\text{cm}^2$, $\sim 13\%$ times larger than that obtained on the Si_3N_4 substrate. However, when pumped above threshold, in contrast to the multimode lasing on Si_3N_4 substrate, the nanowire laser exhibited distinctly different single-mode lasing behavior. Figure 16 shows typical lasing spectra at different pump intensity. The blue curve shows a spectrum when the nanowire was pumped slightly below threshold. Only one dominating peak is seen at 369.3nm . The typical lasing spectra above threshold under different pump intensity are shown as the red and black curves. It is seen as the pump increase, no additional peak appears. We note that the single-mode lasing could be maintained during the increase of the pump power once the threshold was reached. Under a pump intensity of $526\text{KW}/\text{cm}^2$, the single-mode lasing is featured with a side-mode suppression ratio SMSR of 17.4dB and a bandwidth of 0.12nm (via Lorentzian fitting).

4. CONCLUSIONS

We have demonstrated stable, single-frequency output from single, as fabricated nanowire lasers operating far above lasing threshold. Each laser consists of a linear, double-facet GaN nanowire functioning as gain medium and optical resonator. A single-mode linewidth of ~ 0.12 nm and >18 dB side-mode suppression ratio are measured. Crucial to achieving single-mode lasing is reducing the number of cavity modes within the gain bandwidth. This requires significant reduction and precise control of nanowire dimensions, as well as high material gain necessary to compensate for the reduced gain length. These challenges are met using a top-down technique that exploits a tunable dry etch plus anisotropic wet etch. Numerical simulations based on a multimode laser theory indicate that single-mode lasing arises from strong mode competition and narrow gain bandwidth.

We also realized a single-mode GaN nanowire laser by placing two nanowires side-by-side in contact to form a nanowire-pair. The nanowire-pair lased at 370 nm with a threshold of 874 kW/cm² and a SMSR of 15.6 dB was observed. The mode selection of the nanolaser is achieved by the Vernier effect, which in this letter is shown to suppress the multiple transverse mode oscillation as well as multiple longitude mode oscillation of the GaN nanowires. The results indicate a promising approach for transverse-mode selection in nanowires where the nanowire diameter is much larger than the wavelength.

The effect of gold substrate on lasing properties of GaN nanowires is studied. It is found an extra cavity loss can be generated by the substrate, which is highly sensitive to the distributions of different transverse modes. With a controlled nanowire geometry, a mode-dependent loss can be generated to suppress multiple transverse-mode operation and ensure single-mode lasing behavior. Single-mode lasing of ~ 300 nm nanowires on gold substrate is obtained, distinctly different with their multimode lasing behavior on the Si₃N₄ substrates. Our results also indicate that, metal contact may not attenuate the cavity modes strongly for nanowires with large diameters, which offer guidance for design of metal-contacted nanoscale devices.

5. REFERENCES

1. Johnson, J.C., et al., *Single gallium nitride nanowire lasers*. NATURE MATERIALS, 2002. **1**(2): p. 106-110.
2. Chen, L. and E. Towe, *Nanowire lasers with distributed-Bragg-reflector mirrors*. Applied Physics Letters, 2006. **89**(5).
3. Qian, F., et al., *Multi-quantum-well nanowire heterostructures for wavelength-controlled lasers*. NATURE MATERIALS, 2008. **7**(9): p. 701-706.
4. Schlager, J.B., et al., *Steady-state and time-resolved photoluminescence from relaxed and strained GaN nanowires grown by catalyst-free molecular-beam epitaxy*. Journal of Applied Physics, 2008. **103**(12): p. 124309-1-6.
5. Upadhyaya, P.C., et al., *The influence of defect states on non-equilibrium carrier dynamics in GaN nanowires*. Semiconductor Science and Technology, 2010. **25**(2): p. 024017.
6. Hua, B., et al., *Single GaAs/GaAsP Coaxial Core-Shell Nanowire Lasers*. NANO LETTERS, 2009. **9**(1): p. 112-116.
7. Duan, X., et al., *Single-nanowire electrically driven lasers*. Nature, 2003. **421**(6920): p. 241-245.
8. Zimmler, M.A., et al., *Optically pumped nanowire lasers: invited review*. Semiconductor Science and Technology, 2010. **25**(2).
9. Xiao, Y., et al., *Single-Nanowire Single-Mode Laser*. NANO LETTERS, 2011. **11**(3): p. 1122-1126.
10. Scofield, A.C., et al., *Bottom up Photonic Crystal Lasers*. Nano letters, 2011.
11. Li, Q., J.J. Figiel, and G.T. Wang, *Dislocation density reduction in GaN by dislocation filtering through a self-assembled monolayer of silica microspheres*. APPLIED PHYSICS LETTERS, 2009. **94**(23).
12. Li, Q., et al., *Optical performance of top-down fabricated InGaN/GaN nanorod light emitting diode arrays*. Opt. Express, 2011. **19**(25): p. 25528-25534.
13. Sargent, M., M.O. Scully, and J. W. E. Lamb, *Laser Physics* 1991: Addison-Wesley, Heidelberg.
14. Chow, W.W., *Theory of emission from an active photonic lattice*. Physical Review A (Atomic, Molecular, and Optical Physics), 2006. **73**(1): p. 13821-1-13821-13821-9.
15. Chow, W.W., A. Knorr, and S.W. Koch, *Theory of laser gain in group-III nitrides*. Applied Physics Letters, 1995. **67**(6): p. 754-756.
16. van Vugt, L.K., S. Rühle, and D. Vanmaekelbergh, *Phase-correlated nondirectional laser emission from the end facets of a ZnO nanowire*. Nano letters, 2006. **6**(12): p. 2707-2711.
17. Xiao, Y., et al., *Single mode lasing in coupled nanowires*. Applied Physics Letters, 2011. **99**: p. 023109.
18. Gradečak, S., et al., *GaN nanowire lasers with low lasing thresholds*. Applied Physics Letters, 2005. **87**: p. 173111.
19. Ogasawara, N. and R. Ito, *Longitudinal mode competition and asymmetric gain saturation in semiconductor injection lasers. II. Theory*. Japanese journal of applied physics, 1988. **27**(part 1): p. 615-626.

20. Valle, A., J. Sarma, and K. Shore, *Spatial holeburning effects on the dynamics of vertical cavity surface-emitting laser diodes*. Quantum Electronics, IEEE Journal of, 1995. **31**(8): p. 1423-1431.
21. Yang, T., et al., *Optical properties of GaN thin films on sapphire substrates characterized by variable-angle spectroscopic ellipsometry*. Japanese journal of applied physics, 1998. **37**: p. L1105-L1108.
22. Wu, X., et al., *Single mode coupled optofluidic ring resonator dye lasers*. Applied Physics Letters, 2009. **94**: p. 241109.
23. Yeh, C.H., et al., *Stabilized dual-wavelength erbium-doped dual-ring fiber laser*. Optics Express, 2007. **15**(21): p. 13844-13848.
24. Li, Q., et al., *Single-mode GaN nanowire lasers*. Optics Express, 2012. **20**(16): p. 17873-17879.

DISTRIBUTION

1	MS0899	Technical Library	9536 (electronic copy)
1	MS0359	D. Chavez, LDRD Office	1911
1	MS1086	Bob Biefeld	1126(electronic copy)
1	MS1086	Dan Barton	1123(electronic copy)

